Proceedings of the ASME 2013 4th International Conference on Micro/Nanoscale Heat and Mass Transfer
MNHMT2013
December 11-14, 2013, Hong Kong, China

MNHMT2013-22124

TWO-PHASE FLOW AND HEAT TRANSFER IN PIN-FIN ENHANCED MICRO-GAPS WITH NON-UNIFORM HEATING

Steven A. Isaacs
Yogendra Joshi
Yue Zhang
Muhannad S. Bakir
Georgia Institute of Technology
Atlanta, Georgia, USA

Yoon Jo Kim
Washington State University Vancouver
Vancouver, Washington, USA

ABSTRACT

In modern microprocessors, thermal management has become one of the main hurdles in continued performance enhancement. Cooling schemes utilizing single phase microfluidics have been investigated extensively for enhanced heat dissipation from microprocessors. However, two-phase fluidic cooling devices are becoming a promising approach, and are less understood. This study aims to examine two-phase flow and heat transfer within a pin-fin enhanced micro-gap. The pin-fin array covered an area of 1cm x 1cm and had a pin diameter, height and pitch of 150μm, 200μm and 225μm, respectively, (aspect ratio of 1.33). Heating from two upstream heaters was considered. The working fluid used was R245fa. The average heat transfer coefficient was evaluated for a range of heat fluxes and flow rates. Flow regime visualization was performed using high-speed imaging. Results indicate a sharp transition to convective flow boiling mechanism. Unique, conically-shaped two-phase wakes are recorded, demonstrating 2D spreading capability of the device. Surface roughness features are also discussed.

INTRODUCTION

Single phase liquid cooling has shown vast improvements compared to air cooling in microchannels and microgaps. This can be further enhanced through augmentation features such as micro pin fins [1], [2]. While single phase liquid cooling using water provides dramatic performance enhancements, active contact with electronics often requires the coolant to be dielectric. Fluorocarbon fluids and low pressure refrigerants, allow the capability to achieve saturation temperatures closer to desirable chip operating temperatures. Two-phase studies involving dielectric fluids in microchannels have been well represented [3–5]. One of the early studies on flow of a dielectric fluid over micro pin fin arrays looked at single-phase cooling, and flow boiling [6]. Using a 1800μm x 10000μm array of 100μm diameter staggered fins and gap height of 243μm, results indicated Nusselt Number values greater than 20 using R-123 as working fluid. Recent micro channel studies have reported that low pressure, two-phase refrigerant systems can dissipate heat loads as high as 350 W/cm^2 [7].

This study aims to broaden the experimental knowledge base of two-phase flow over micro pin fin array populated microgaps. Current literature only supports micro pin fin arrays placed in relatively narrow channels (2mm x 1cm), while there is no literature supporting studies on micro pin fin enhanced micro-gaps placed on larger, chip-sized areas (1cm x 1cm). Also, the particular working fluid used in this study, R245fa, has yet to be studied for this type of scale and surface enhancement geometry.

KEY WORDS: two-phase, micro-gap, pin fin

NOMENCLATURE

A	area (m^2)
c	temperature coefficient (/^{o}C)
h	enthalpy (kJ/kg) or heat transfer coefficient (W/m^{2}K)
$\dot{m}$	mass flowrate (kg/s)
q	heat load (W)
R	electrical resistance (Ω)
T	temperature (K)
x	vapor quality (-)

Greek symbols

η	fin efficiency
Δ	change in

Subscripts

b	array base
b_{exp}	base exposed
eff	effective
f	fin
f_{exp}	fin exposed
f_{out}	outlet fluid
g_{out}	vapor outlet

in	inlet
o	reference value
out	outlet
w	wall
∞	fluid reference

EXPERIMENTAL SETUP

The experimental platform used in this study consisted of a cleanroom fabricated, silicon, pin fin sample and a closed, flow loop. The micro pin fin sample had etched, silicon, cylindrical fins. The extended surfaces were populated on a 1cm x 1cm square surface that included inlet and outlet flow passages. The height, pitch and diameter of the pins were 200µm, 225µm, and 150µm, respectively (Figure 1). The pins were located in 43 rows with 42 pins per row. To simulate heating, four platinum heaters were deposited on the backside of the sample directly behind the pin fin array.

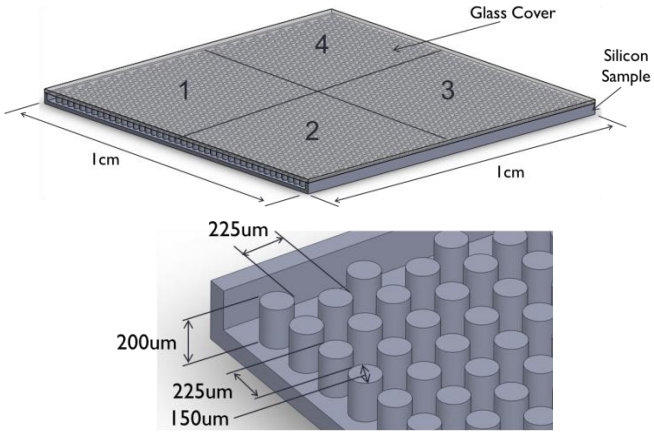

Figure 1. Pin Fin Array Diagram

A clear glass cover was bonded with epoxy to the top of the pin fin array. This had two main purposes. The first was to completely seal the pins and flow passages. The second was to provide a means of visualizing flow through the sample during experimental runs. Inlet/Outlet ports mounted on the back of the sample corresponding to the inlet and outlet passages allowed for connections to the refrigerant flow loop. A printed circuit board (PCB) was included in the device setup in order to facilitate wiring from the sample's copper pads to power supplies (Figure 2). SEM images can be seen in Figure 3.

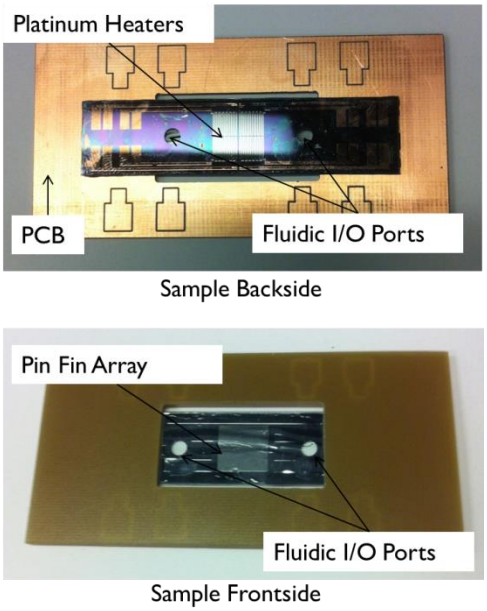

Figure 2. Pin Fin Device

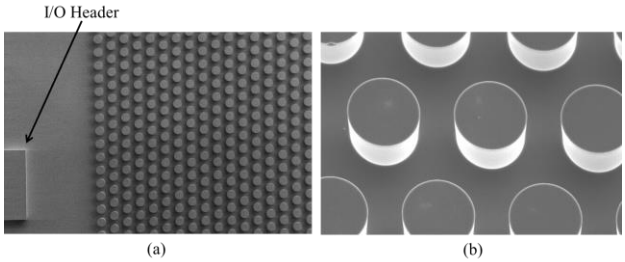

Figure 3. SEM images of samples

The refrigerant flow loop constructed to measure the pressure drop and heat transfer characteristics across the pin fin sample can be seen in Figure 4. This setup consisted of a primary refrigerant loop and secondary cooling loop. The primary loop was composed of a pump, flowmeter, two heat exchangers, metering valve and a pre-heater connected with insulated ¼" copper tubing. The secondary loop simply supplied chilled water to the backside of the copper heat exchangers. All tubing and components were encased in foam insulation. A Cole-Palmer digital magnetic gear pump and a McMillan microturbine flowmeter with a 20-200 ml/min measurement range were used. The copper heat exchangers assisted in heat removal downstream of the pin fin sample and before the pre-heater. The pre-heater and metering valve were located directly upstream of the pin fin sample and allowed for temperature and pressure control based on the degree of prescribed subcooling. Swagelok brass inline 15 micron-sized element pores provided means of filtering the working fluid. Pressure and temperature measurements were taken at the inlet and outlet of the pin fin sample. Uncertainties associated with the pressure transducers and T-type thermocouples were 0.25% FS and 0.5°C. Table 1 shows uncertainties in experimental

measurements. Propagation of uncertainty analysis was used to determine uncertainty of calculated results.

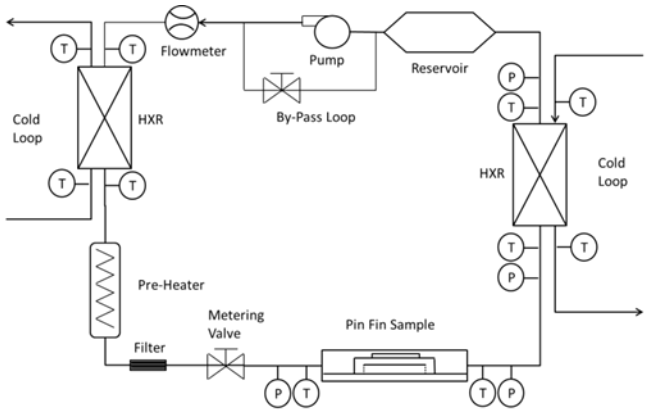

Figure 4. Flow loop diagram

Table 1. Experimental uncertainties

Quantity	**± Uncertainty**
I/O temperature, T (°C)	0.5 °C
I/O pressure, P (kPa)	0.25% FS
Mass flux, G (kg/m^{2}s)	3%
Current (A)	0.2%
Voltage (V)	0.2%
Fin height (μm)	3%
Sample length (cm)	2%
Sample width (cm)	2%
Heat transfer coefficient, h (W/m^{2}K)	9-24%

The pin fin sample was connected to the refrigerant loop via clear vinyl tubing. Insulation was wrapped around the sample and clear tubing. Small sections of the tubing directly before and after the inlet/outlet ports were exposed to serve as viewing windows of the flow before and after the pin fin sample.

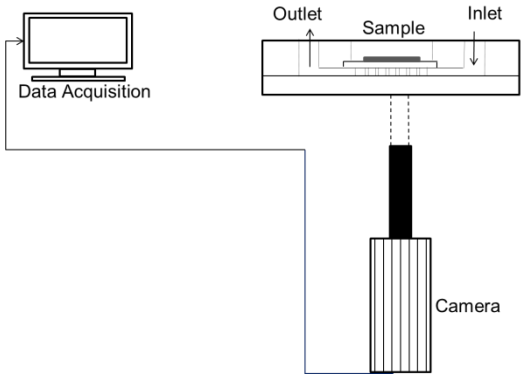

Figure 5. Flow visualization system

EXPERIMENTAL PROCEDURE

To begin the experiments, the system pump was used to run refrigerant R245fa through the primary loop and chilled water was run through the secondary loop side of the heat exchangers. Subcooling was held between 10 and 13 °C for this study. The system was allowed to reach steady state for each test point. Steady state was defined as an experimental condition in which changes in temperature and pressure measurements were less than the associated uncertainties. Tests began with single phase conditions. As heat flux from the heaters was increased, the system transitioned to two-phase flow conditions. Heat flux was increased until the inlet pressure reached levels nearing the point at which the sample was known to fracture (determined by pressure tests to be ~300kPa).

This particular study involved the active use of the two upstream heaters (heaters 1 and 2 in Figure 1). With mass flux held at 888 kg/m^{2}s total heat flux was gradually stepped from 14 to 39.3 W/cm^2 (equal power to each heater). Data was acquired at 1Hz. Once the system reached steady state, data was collected and averaged across that particular heat flux. Flow visualization was simultaneously run at a frame rate of 2000 fps to capture high-speed video of the flow over the pin fin array.

DATA REDUCTION

The power into the flowing refrigerant, q_{eff}, was calculated from.

$$q_{eff} = q_{total} - q_{loss} \quad (1)$$

where the heat loss, q_{loss}, was calculated from single phase experiments through an energy balance.

Each run involved the determination of heat transfer coefficient, h, which was calculated using the fin efficiency model [8]. Since the bonding technique used could not guarantee a zero tip clearance between the fin and glass cover, the adiabatic fin tip condition was used with a corresponding corrected length. From here, an iterative approach was used to obtain the average heat transfer coefficient for each case shown by the diagram in Figure 6.

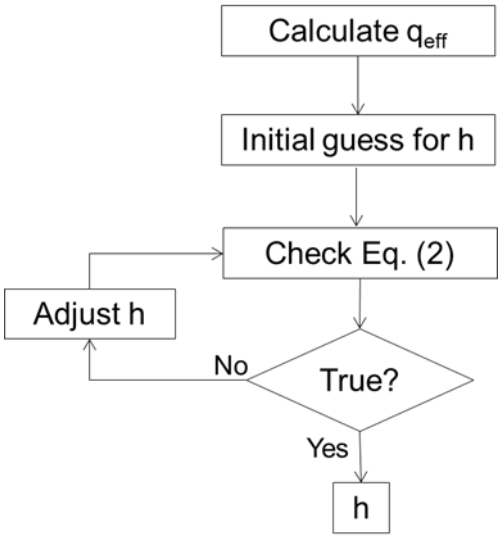

Figure 6. Flow diagram of iterative method

The effective power into the fluid stream was expressed as

$$q_{eff} = h\left(A_{b_{ezp}} + \eta A_{f_{exp}}\right)(T_w - T_\infty) \quad (2)$$

where the value of T_∞ was dependent on the flow phase. For single phase conditions, T_∞ was the average temperature of the fluid across the array. For two-phase conditions, T_∞ was the saturation temperature of the fluid based on the average pressure across the array. Pressure drops through fittings and tubing between the sample and pressure/temperature measurements locations were calculated and determined to be less than 3% compared to the pressure drop across the array, and were neglected.

Base temperatures of the array were calculated using the integrated Platinum heaters through the equation

$$R(T) = R_o(1 + c\Delta T) \quad (3)$$

where c was the temperature coefficient of the individual heater determined through calibration. For the heaters used in this study, the temperature coefficient values were 0.002975 and 0.002809/ºC.

Exit enthalpy was determined through an energy balance

$$q_{eff} = \dot{m}(h_{out} - h_{in}) \quad (4)$$

Since the inlet was maintained subcooled, h_{in} was calculated as the fluid enthalpy entering the sample. Vapor quality at the outlet of the sample was then determined by

$$x = (h_{out} - h_{f_{out}}) \,/\, (h_{g_{out}} - h_{f_{out}}) \quad (5)$$

RESULTS

Figure 7 displays average heat transfer coefficient with increasing heat flux. Single phase flow is identified via flow visualization at relatively low heat flux. In this region heat transfer coefficient decreases due to an increase in base temperature of the upstream heaters. Near a heat flux of 19 W/cm^2 as heat flux is steadily increased, a sharp jump in heat transfer coefficient is seen due to initiation of flow boiling over the array. This is then followed by a steep decrease in heat transfer coefficient, eventually reaching a steady decline at 30 W/cm^2.

Similar to Kosar and Peles [9], after reaching its maximum value, the heat transfer coefficient decreases with increasing heat flux, which is attributed to the convective boiling mechanism. In the literature, the heat transfer coefficient gradually increases from single-phase up to the maximum value in this partial boiling region. In this study, however, a rapid jump in heat transfer coefficient is recorded from single to two-phase conditions over a relatively small heat flux change of 4W/cm^2. Immediately after this jump, the two-phase flow region is distributed as shown in the first image of Figure 11. It is determined that since the heat transfer coefficient only decreases during the two-phase portion of the tests, the data suggests that the dominant flow boiling mechanism is convective flow boiling, while nucleate boiling associated with an increase in heat transfer coefficient for increasing heat flux is nonexistent. Figure 8 compares the two-phase data of the current study to the convective boiling correlation of Peles and Kosar [9]. This correlation is in reasonable agreement with the data with the largest discrepancy occurring at the initiation of two-phase flow.

Figures 9 and 10 display heat transfer coefficient data for a range of flowrates for a study under two-phase conditions. Very little deviation in heat transfer coefficient exists between the different flowrates. Error ranges overlap indicating very little dependence on flowrate.

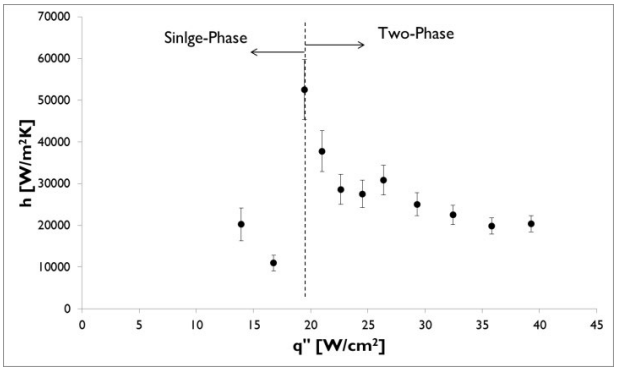

Figure 7. h vs. q'' at G = 888 kg/m^{2}s

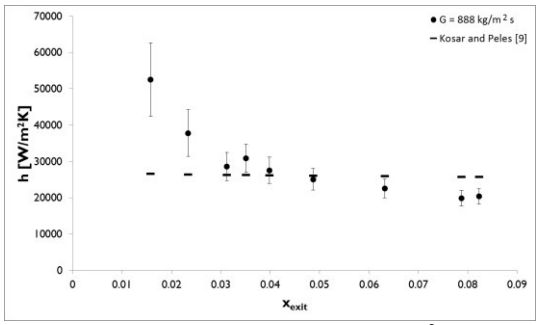

Figure 8. h vs. x_e G = 888 kg/m^{2}s

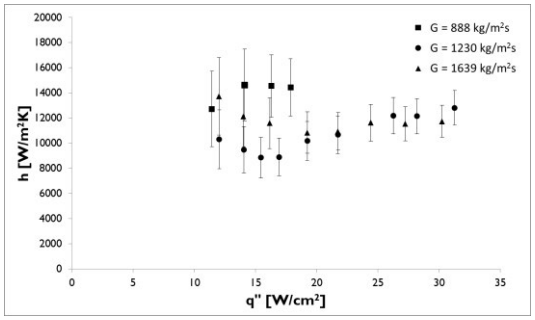

Figure 9. h vs. q'' for a range of flowrates

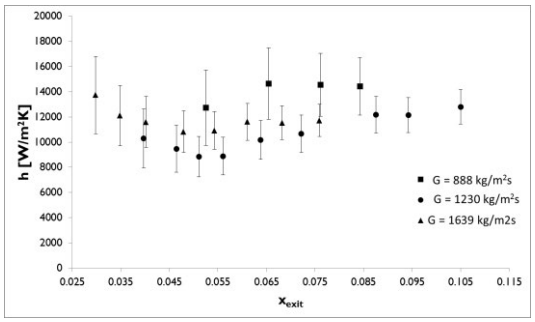

Figure 10. h vs. x_e for a range of flowrates

The first image in Figure 11 indicates locations of heaters 1 and 2 (upstream heaters). Unlike the array area associated with heater 2, a large two-phase region covers a majority of the heater 1 area. This is considered to be a consequence of surface roughness differences between these two areas since the power supplied to each heater is constant. Conically-shaped wakes can be seen forming downstream of bubble departure points. This demonstrates the two-dimensional spreading of flow, as is characteristic with this type of pin fin enhancement [10]. These unique wake structures continue to grow and merge until a majority of the array is blanketed by a two-phase region at 39.3 W/cm^2. This is believed to be a consequence of conduction from the upstream heaters to the downstream base of the array for increasing heat flux.

A brief investigation of bubble formation was performed. Bubble formation was seen to occur under two different surface conditions: formation on individual pins and formation at surface roughness features. Figure 12 displays image capture of both types of bubble formation. Clear bubble formation occurs at what is suspect to be a small scratch at the base of the array in image (a). Formation at pin surfaces varied under identical experimental parameters while formation at surface roughness features was consistent.

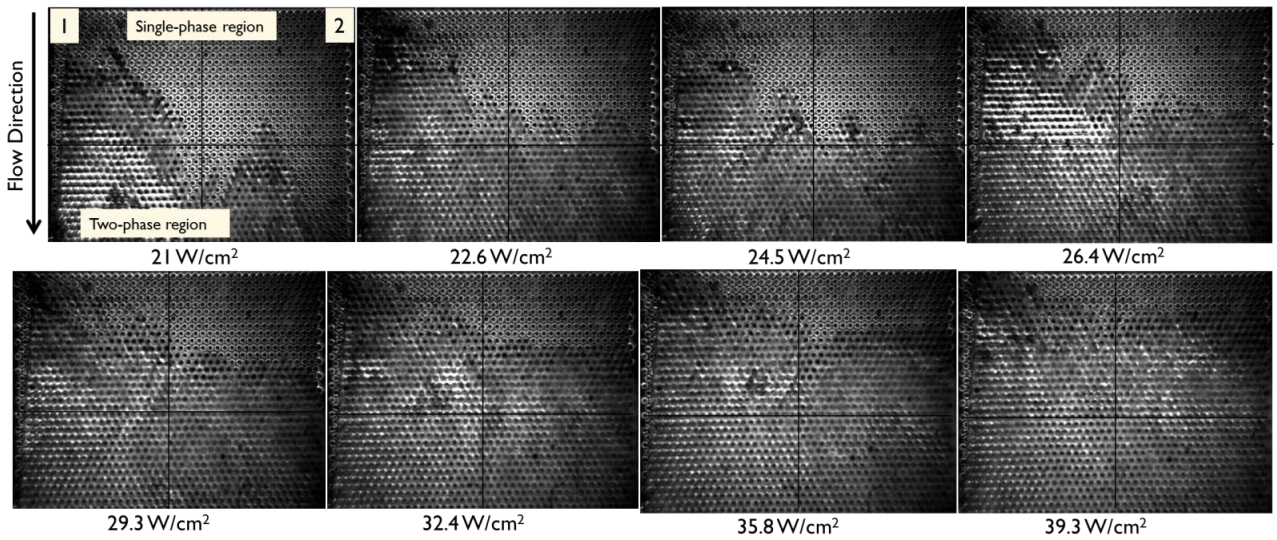

Figure 11. Flow visualization performed at a frame rate of 2000 fps

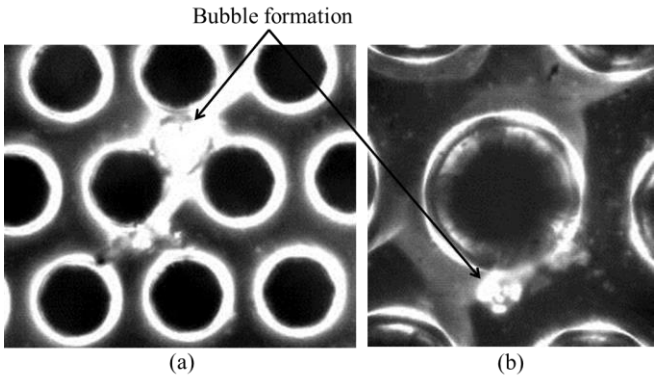

Figure 12. Bubble formation at a) surface roughness feature and b) pin surface

CONCLUSION

In this study an experimental evaluation of a pin fin enhanced micro-gap was performed. Heat transfer coefficient values, along with supporting flow visualization data were presented. The primary conclusions of this study are listed below:

- A much sharper increase in heat transfer coefficient during the single-phase/two-phase transition.
- Data supports the inference that the dominant flow boiling mechanism is convective boiling and this matches well with the relevant correlation.
- Surface roughness effects may play a vital role in phase transition in terms of two-phase wake location and size.
- Evolution in two-phase wakes from conical structures to array-encompassing blankets demonstrates two-dimensional effects of pin fin enhanced micro-gaps.

REFERENCES

[1] P.-S. Lee and S. V. Garimella, "Saturated Flow Boiling Heat Transfer and Pressure Drop in Silicon Microchannel Arrays," *International Journal of Heat and Mass Transfer*, vol. 51, no. 3–4, pp. 789–806, Feb. 2008.

[2] W. Qu and A. Siu-Ho, "Experimental Study of Saturated Flow Boiling Heat Transfer in an Array of Staggered Micro-Pin-Fins," *International Journal of Heat and Mass Transfer*, vol. 52, no. 7–8, pp. 1853–1863, Mar. 2009.

[3] B. Agostini, J. R. Thome, M. Fabbri, B. Michel, D. Calmi, and U. Kloter, "High Heat Flux Flow Boiling in Silicon Multi-Microchannels – Part I: Heat Transfer Characteristics of Refrigerant R236fa," *International Journal of Heat and Mass Transfer*, vol. 51, no. 21–22, pp. 5400–5414, Oct. 2008.

[4] B. Agostini, J. R. Thome, M. Fabbri, B. Michel, D. Calmi, and U. Kloter, "High Heat Flux Flow Boiling in Silicon Multi-Microchannels – Part II: Heat Transfer Characteristics of Refrigerant R245fa," *International Journal of Heat and Mass Transfer*, vol. 51, no. 21–22, pp. 5415–5425, Oct. 2008.

[5] J. R. Thome, "Boiling in Microchannels: A Review of Experiment and Theory," *International Journal of Heat and Fluid Flow*, vol. 25, no. 2, pp. 128–139, Apr. 2004.

[6] A. Koşar and Y. Peles, "Convective Flow Of Refrigerant (R-123) Across A Bank Of Micro Pin Fins," *International Journal of Heat and Mass Transfer*, vol. 49, no. 17–18, pp. 3142–3155, Aug. 2006.

[7] J. E. Park and J. R. Thome, "Critical Heat Flux in Multi-Microchannel Copper Elements with Low Pressure Refrigerants," *International Journal of Heat and Mass Transfer*, vol. 53, no. 1–3, pp. 110–122, Jan. 2010.

[8] F. P. Incropera, D. P. DeWitt, T. L. Bergman, and A. S. Lavine, *Fundamentals of Heat and Mass Transfer*, vol. 6th. John Wiley & Sons, 2007, p. 997.

[9] A. Koşar and Y. Peles, "Boiling Heat Transfer In A Hydrofoil-Based Micro Pin Fin Heat Sink," *International Journal of Heat and Mass Transfer*, vol. 50, no. 5–6, pp. 1018–1034, Mar. 2007.

[10] S. A. Isaacs, Y. J. Kim, A. J. McNamara, Y. Joshi, Y. Zhang, and M. S. Bakir, "Two-Phase Flow and Heat Transfer in Pin-Fin Enhanced Micro-Gaps," *13th InterSociety Conference on Thermal and Thermomechanical Phenomena in Electronic Systems*, pp. 1084–1089, May 2012.